# Ni:ZnO Nanostructures, Effect of Ni Content on Size and Strain

Durga Prasad Gogoi
*Department of Physics, Namrup College*
*Dibrugarh , Assam, India, 786623*

**Abstract- Ni doped ZnO nanostructure is studied extensively to explore its structural behavior. Solid state chemical reaction route is utilized to fabricate the nanostructures. Formation of nanorods has been visualized by applying HRTEM. Concentration of Ni content in ZnO host lattice is the main parameter for experimental investigation. Investigation reveals that the crystallite size of the Ni doped ZnO slightly decreases due to Ni doping compared to undoped specimen. Study shows that with decreasing size of nanostructures strain also decreases.**

**Keywords – Ni, Nanorods, ZnO, HRTEM**

## I. INTRODUCTION

Among the transition metal, Ni is an important dopant; since, $Ni^{2+}$ (0.69 A°) has the same valence as $Zn^{2+}$and its radius is close to that of Zn+ (0.74 A°), so it is possible for $Ni^{2+}$ to replace $Zn^{2+}$ in ZnO lattice. So far, the influence of Ni doping in the ZnO lattice host has been reported by several groups. Doping of Ni in ZnO matrix has been done by several techniques [1-4], we have fabricated Ni doped ZnO nanpstructures by adopting the solid state chemical reaction route as described in earliar works [5, 6]. The concentration of Nickel acetate and Zinc acetate were varied within the range 1 at% Ni - 5 at% Ni and accordingly indexed as Ni-1, N-3 and Ni-5. In this paper the structural properties are discussed. XRD. EDS. HRTEM were carried out to investigate structural properties of Ni:ZnO nanostructures. XRD study ruled out the existence of additional phases in the sample due to Ni doping. HRTEM study showed the clear evidence of formation nanorods for Ni:ZnO system.

## II. EXPERIMENTAL

### *A. X- ray diffraction study*

Ni doped samples (Ni-1, Ni-3 and Ni-5) exhibit hexagonal wurtzite structure of ZnO in their XRD patterns presented in figure 1. The XRD pattern reveals the absence of any secondary phases due to Ni doping. Compared to undoped specimen Ni doped samples exhibit peak shift in the XRD spectra. The XRD peak shift for the Ni:ZnO system can be more clearly visualized from the figure:2, which is obtained by plotting from the XRD data within the '2θ' range $31^o$-$37^0$ for the reflections by the planes (100), (002) and (101). The values for '2θ' at the peak positions corresponding to the diffracting planes (1 0 0), (0 0 2) and (1 0 1) for the samples (ZnO, Ni-1, Ni-3 and Ni-5) are presented in the table: 1. Different values for '2θ' corresponding to a particular peak clearly indicates the peak shift. The shift of peaks for the Ni doped samples take place towards the higher value of '2θ' from the peak positions for pure ZnO sample. The change of XRD peak can be attributed for the change of size and strain of the Ni:ZnO nanostructures due to Ni doping.

The lattice spacing 'd' for all samples were estimated from their respective '2θ' values corresponding to the diffracting planes (1 0 0), (0 0 2) and (1 0 1) of the nanocrystals which are shown in the table: 1. From the table 'd' values were utilizes to estimate the lattice parameters 'a' and 'c' as 3.237 Å and 5.2 Å respectively.

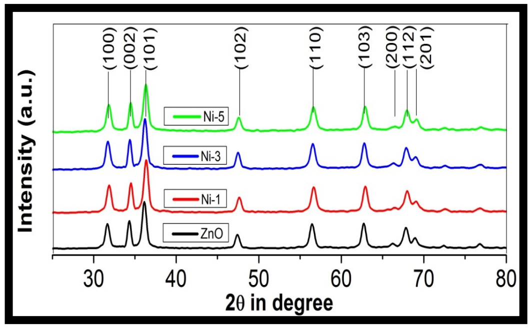


Figure 1. XRD pattern of bare ZnO and Ni doped ZnO for three Ni samples.

For determination of size of the nanostructures, FWHM and 2θ values corresponding to the most intense peak (1 0 1) were considered for the Scherer formula and the respective values are presented in the table: 1. From the estimated size, we have observed that the crystallite size of the Ni doped ZnO slightly decreases due to Ni doping compared to undoped specimen. The size of the nanocrystals lies within the range 14.1 nm – 15.51 nm.

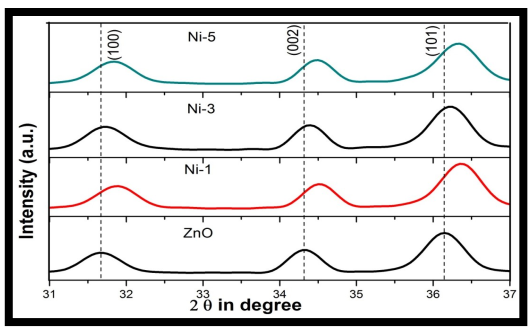


Figure 2. Enlarged view of the XRD pattern for the samples (ZnO, Ni-1, Ni-3 and Ni-5) within diffraction angle (2θ) range 31° - 37° corresponding to the reflecting planes (100), (002) and (101), showing clear peak shift.

Table -1 '2θ' values corresponding to the peak positions for diffracting planes (1 0 0), (0 0 2) and (1 0 1) for the samples ZnO and Ni:ZnO

| Plane | ZnO | Mn-1 | Mn-3 | Mn-5 |
|---|---|---|---|---|
| (1 0 0) | 31.68 | 31.87 | 31.72 | 31.83 |
| (0 0 2) | 34.32 | 34.5 | 34.39 | 34.48 |
| (1 0 1) | 36.14 | 36.36 | 36.22 | 36.33 |

Table -2 Lattice spacing for the diffracting planes (1 0 0), (0 0 2) and (1 0 1) for the samples (ZnO, Ni-1, Ni-3 and Ni-5) estimated from their respective '2θ' values as shown in table: 1.

| | ( 'd' spacing in Å) | | | |
|---|---|---|---|---|
| | ZnO | Ni-1 | Ni-3 | Ni-5 |
| (1 0 0) | 2.82 | 2.81 | 2.82 | 2.8 |
| (0 0 2) | 2.61 | 2.6 | 2.6 | 2.6 |
| (1 0 1) | 2.48 | 2.47 | 2.48 | 2.47 |

Table -3 Estimated crystallite size of as synthesized nanostructures for the samples (ZnO, Ni-1, Ni-3 and Ni-5) estimated from FWHM and 2θ values corresponding to (101) diffracting plane of each sample.

| | FWHM (w) (degree) | 2θ (degree) | crystallite size (nm) |
|---|---|---|---|
| ZnO | .53254 | 36.14 | 15.51 |
| Ni-1 | .55806 | 36.36 | 14.81 |
| Ni-3 | .54001 | 36.22 | 15.3 |
| Ni-5 | .5863 | 36.33 | 14.1 |

The size and strain of the nanostructures were also estimated from Williamson-Hall (W-H) plot as shown in figure: 3 for the sample Ni-5. In this plot the first six peaks of the XRD pattern have been considered. From the intercept (~0.0099) and the slope (~ 7.488 x $10^{-4}$) of the plot the average size and strain of the Ni-5 nanostructures were estimated. In a similar way the size and strain of other samples were also estimated and presented in the table- 4.

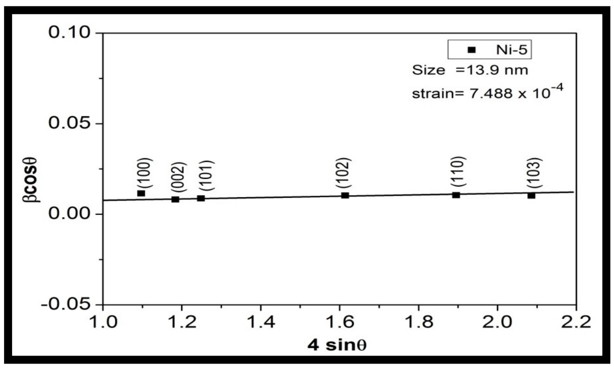


Figure 3. Williamson- Hall plot for the sample Ni-5, from the slope and intercept of the straight line strain (7.488 x $10^{-4}$) and size (13.9 nm) of the Ni-5 nanostructures were estimated.

Table -4 Crystallite size and strain estimated from Williamson- Hall plot for the samples (ZnO, Ni-1, Ni-3 and Ni-5)

| sample | size (nm) | strain |
|---|---|---|
| ZnO | 16.17 | 2.58 X $10^{-3}$ |
| Ni-1 | 15.75 | 1.14 X $10^{-3}$ |
| Ni-3 | 15.9 | 1.44 X $10^{-3}$ |
| Ni-5 | 13.9 | 0.75 X $10^{-3}$ |

*B. Transmission electron microscopy study*

HRTEM study revealed the formation of nanorods with average length 44.5 nm and diameter 12 nm as observed in figure: 4A and 4B. Figure: 4C represents the SAED pattern focused on the isolated nanorod of av. length 56 nm and av. diameter 14 nm (inset of figure: 4C). The lattice spacing 0.22 nm has been observed from the HRTEM image (figure: 4D) of the isolated nanorod as shown in the inset of figure: 4C. Clear lattice fringe pattern can be attributed due to the high crystalline nature of the as synthesised sample. In case of Ni-5, it is observed a large number of isolated nanorods. In this concentration of Ni the growth plane was confirmed along the (101) plane.

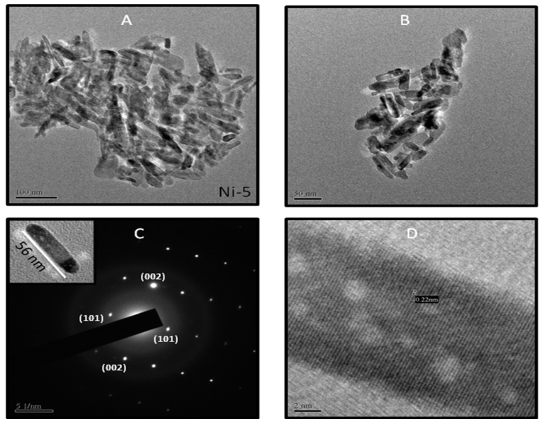


Figure 4. TEM image of Ni-5 showing formation of elongated nanostructures. Figure (A) and (B) depicts formation of nanorods with av. length 44.5 nm and av. diameter 12 nm. For the sample Ni-5, (C) SAED pattern, Inset : an isolated nanorod of av. length 56 nm and av. diameter 14 nm, (D) HRTEM image, when beam was focussed on the isolated nanorod; showing lattice spacing 2.2 Å,.

## IV.CONCLUSION

From the above investigations it has been noticed that with decreasing size of the nanostructures the strain also decreases. The highest stain was exhibited by ZnO nanorod with size 16.17 nm, while the lowest strain was shown by Ni-5 with size 13.9 nm. The particle size, as obtained from both XRD data is in agreement with the sizes as calculated from W-H plot. This may be due to the limitations of Scherrer formula where particle strain is not considered. It was observed that along with decrease in size, the strain also decreases. Thus, size and strain of the nanostructures can be simultaneously manipulated by changing doping concentration. HRTEM study for all samples exhibited clear fringe patterns; it was attributed due to high crystalline nature of the as-synthesised samples. The growth direction of the bare ZnO was found along (102), while for all Ni doped samples it was found along (101) plane.

## REFERENCES

[1] Yin, Z., et al. Structural, magnetic properties and photoemission study of Ni-doped ZnO, *Solid Stat. Commun*. **135**, 430 - 433, 2005.

[2] Wang, X.B., et al. The influence of different doping elements on microstructure, piezoelectric coefficient and resistivity of sputtered ZnO film, *Appl. Surf. Sci.* **253**, 1639 - 1643, 2006.

[3] Cheng, C.W., Xu, G.Y., Zhang, H.Q., Luo, Y. Hydrothermal synthesis Ni-doped ZnO nanorods with room-temperature ferromagnetism, *Mater. Lett*. **62**, 1617, 2008.

[4] S. Ghosh, S., et al. Study of ZnO and Ni-doped ZnO synthesized by atom beam sputtering technique, *Appl. Phys. A* **90**, 765 - 769, 2008.

[5] D. P. Gogoi, Structural and Spectroscopic Investigations of Mn doped Nanorods pp.433-441, *International Journal of Nanotechnology and Applications,* ISSN 0973-631X

[6] D. P. Gogoi, Structural Investigation of ZnO Nanostructures*, International Journal of Latest Trends in Engineering and Technology* Vol(15) Issue(2), pp-044-047, e-ISSN:2278-621X